PROPAGATION OF PLANE SURFACE WAVES OVER A RECTANGULAR STEP WITH OVERHANG AND OVER A PARTIALLY CAPPED RECTANGULAR TRENCH

I. V. Sturova UDC 532.59

The scattering of surface waves by various bottom irregularities is a classical problem in wave hydrodynamics. However, obstacles with shadow zones, where the shape of the irregularity is a multiple-valued function of the horizontal coordinates, have not been considered to date. For our investigation we have chosen the simplest bottom irregularities shape: a step with an overhang, and a partially capped trench. We consider the plane potential wave motion of a ideal incompressible fluid in the linear problem. We investigate the influence of the bottom geometry on the characteristics of the reflected and transmitted waves and on the kinetic energy of the fluid in the pocket formed in the bottom. To solve the method numerically, we use the method of integral matching along vertical segments partitioning the entire flow region into rectangular subregions. This method has been used to investigate the action of waves on an underwater rectangular obstacle [1] and in application to an ordinary rectangular trench [2, 3], in one case [3] where a denser fluid layer is situated inside the trench. The propagation of waves over a step has also been investigated [4] using the conventional matching technique.

1. Let a fluid occupy a domain S bounded by a free surface and a rigid impenetrable bottom. In the case of a step, H_1 is the depth of the fluid to the left of it, H_2 is the depth to the right ($H_2 > H_1$), and ℓ is the length of the horizontal, rigid, infinitely thin overhang AB (Fig. 1a). The coordinate system is chosen so that the x axis coincides with the unperturbed level of the free surface, and y passes through the end of the overhang (point B) and is directed upward. The motion of the fluid is assumed to be potential everywhere except at corner points, in the neighborhood of which the velocity goes to infinity of the order $r^{(\theta-\pi)/(2\pi-\theta)}$ (r is the distance from the corner point, and θ is the angle for a rigid body).

The incident waves propagate in the positive x direction from the shallow-water to the deep-water part of the fluid and are described by the velocity potential $\Phi_0(x, y, t) = \phi_0(x, y)\exp(-i\sigma t)$, where $\varphi_0 = \dfrac{iag \operatorname{ch} k_1(y+H_1)}{\sigma \operatorname{ch} k_1 H_1}\exp(ik_1x)$; a and σ are the amplitude and frequency of the wave, and the wave number k_1 is determined from the equation

$$\sigma^2 = gk_1 \operatorname{th} k_1H_1 \tag{1.1}$$

(g is the acceleration of gravity). Here and in all other expressions containing the factor $\exp(-i\sigma t)$, only the real part has physical significance.

We consider steady-state waves and seek the velocity potential of the total perturbed flow in the form $\Phi(x, y, t) = \phi(x, y)\exp(-i\sigma t)$. In order to determine the function $\phi(x, t)$, it is necessary to solve the problem

$$\begin{gathered}\Delta\varphi = 0\ (x,\ y \in S),\\ \sigma^2\varphi - g\partial\varphi/\partial y = 0\ (y = 0),\ \partial\varphi/\partial n = 0 \text{ (on the bottom contour)}\end{gathered} \tag{1.2}$$

(n is the normal to the bottom line). The reflected and transmitted waves must satisfy the radiation conditions in the limit $|x| \to \infty$.

The problem (1.2) is solved by a matching technique similar to the one used in [3]. The region S is partitioned into three rectangular subregions: $S_1 = [-\infty < x < 0, -H_1 \le y \le 0]$; $S_2 = [0 < x < \infty, -H_2 \le y \le 0]$; $S_3 = [-\ell < x < 0, -H_2 \le y \le -H_1]$; in the j-th subregion

Novosibirsk. Translated from Zhurnal Prikladnoi Mekhaniki i Tekhnicheskoi Fiziki, No. 5, pp. 40-46, September-October, 1991. Original article submitted February 6, 1990; revision submitted June 19, 1990.

 0021-8944/91/3205-0684$12.50

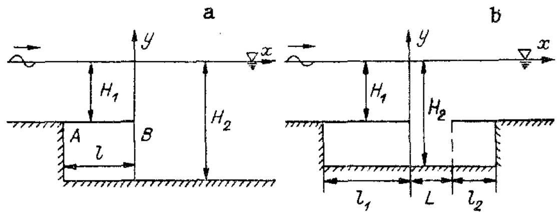

Fig. 1

(j = 1, 2, 3) the function $\phi(x, y)$ is denoted by $\phi_j(x, y)$. Since the motion of the fluid is continuous in S, conditions are established at the boudnaries of the subregions S_j for matching of the pressure and the horizontal velocity along the vertical line x = 0; it follows from these conditions that

$$\begin{gathered}\varphi_1 = \varphi_2,\ \partial\varphi_1/\partial x = \\ = \partial\varphi_2/\partial x\ (-H_1 \leqslant y \leqslant 0), \\ \varphi_3 = \varphi_2,\ \partial\varphi_3/\partial x = \\ = \partial\varphi_2/\partial x\ (-H_2 \leqslant y \leqslant -H_1).\end{gathered} \tag{1.3}$$

Invoking the separation of variables, we seek the functions ϕ_j in the form of expansions in eigenfunctions of the corresponding boundary-value problems:

$$\varphi_1 = \varphi_0 + A_0 \exp(-ik_1x)\,Y_1(y) + \sum_{n=1}^{\infty} A_n \exp(k_{1n}x)\,Y_{1n}(y), \tag{1.4}$$

$$\varphi_2 = B_0 \exp(ik_2x)\,Y_2(y) + \sum_{n=1}^{\infty} B_n \exp(-k_{2n}x)\,Y_{2n}(y),$$

$$\varphi_3 = C_0 + \sum_{m=1}^{\infty} C_m \cos\beta_m(y + H_1)\operatorname{ch}\beta_m(x + l).$$

Here $\beta_m = m\pi/h$, $h = H_2 - H_1$, and k_{1n} (n = 1, 2, ...) are the roots of the equation

$$\sigma^2 = -gk \operatorname{tg} kH_1. \tag{1.5}$$

The quantities k_2 and k_{2n} are determined from Eqs. (1.1) and (1.5) with H_1 replaced by H_2. The eigenfunctions Y_1, Y_{1n} and Y_2, Y_{2n} are orthogonal and are normalized as follows:

$$Y_1(y) = \frac{\operatorname{ch} k_1(y + H_1)}{\sqrt{\Lambda_1}},\quad \Lambda_1 = \int_{-H_1}^{0} \operatorname{ch}^2 k_1(y + H_1)\,dy,$$

$$Y_{1n}(y) = \frac{\cos k_{1n}(y + H_1)}{\sqrt{\Lambda_{1n}}},\quad \Lambda_{1n} = \int_{-H_1}^{0} \cos^2 k_{1n}(y + H_1)\,dy,$$

$$Y_2(y) = \frac{\operatorname{ch} k_2(y + H_2)}{\sqrt{\Lambda_2}},\quad \Lambda_2 = \int_{-H_2}^{0} \operatorname{ch}^2 k_2(y + H_2)\,dy,$$

$$Y_{2n}(y) = \frac{\cos k_{2n}(y + H_2)}{\sqrt{\Lambda_{2n}}},\quad \Lambda_{2n} = \int_{-H_2}^{0} \cos^2 k_{2n}(y + H_2)\,dy.$$

The reduction method is used to replace the infinite series in Eqs. (1.4) by finite sums with N and M terms, respectively. The unknown complex constants A_0, B_0 and A_n, B_n, C_m (n = 1, ..., N; m = 1, ..., M) are determined from the matching conditions (1.3), which are satisfied in the integral sense:

$$ik_2B_0 = \int_{-H_1}^{0} \frac{\partial\overline{\varphi}_1}{\partial x} Y_2\,dy + \int_{-H_2}^{-H_1} \frac{\partial\overline{\varphi}_3}{\partial x} Y_2\,dy,$$

$$-k_{2n}B_n = \int\limits_{-H_1}^{0} \frac{\partial\bar{\varphi}_1}{\partial x} Y_{2n}\,dy + \int\limits_{-H_2}^{-H_1} \frac{\partial\bar{\varphi}_3}{\partial x} Y_{2n}\,dy \quad (n = 1, \ldots, N),$$

$$A_0 = \int\limits_{-H_1}^{0} \bar{\varphi}_2 Y_1\,dy - \int\limits_{-H_2}^{0} \varphi_0 Y_1\,dy, \quad A_n = \int\limits_{-H_1}^{0} \bar{\varphi}_2 Y_{1n}\,dy \quad (n = 1, \ldots, N),$$

$$C_m = \frac{2}{h \operatorname{ch} \beta_m l} \int\limits_{-H_2}^{-H_1} \bar{\varphi}_2 \cos\beta_m (y + H_1)\,dy \quad (m = 1, \ldots, M) \tag{1.6}$$

[$\bar{\phi}_j$ denotes the finite sums in the corresponding series (1.4) of the function $\phi_j(0, y)$].

The integrals in Eqs. (1.6) are expressed in terms of elementary functions. The linear system (1.6) of 2 + 2N + M equations is conveniently reduced to a system of 2 + 2N equations by eliminating the constants C_m. The resulting system is solved numerically by the Gaussian method.

The most interesting wave diffraction characteristics are the reflection coefficient R and the transmission coefficient T, which are equal to the ratios of the amplitudes of the reflected and transmitted waves, respectively, to the amplitude of the incident wave and, according to Eq. (1.4), are given by the expressions

$$R = \frac{\sigma \operatorname{ch} k_1 H_1}{ag\sqrt{\Lambda_1}} |A_0|, \quad T = \frac{\sigma \operatorname{ch} k_2 H_2}{ag\sqrt{\Lambda_2}} |B_0|.$$

We know from the general theory of the propagation of linear plane waves over a rough bottom [5] that the following relation holds by the energy conservation law for a fluid whose depths tends to constant values H_2 and H_1 in the limit $x \to \pm\infty$:

$$R^2 + \frac{S(k_2H_2)}{S(k_1H_1)} T^2 = 1, \tag{1.7}$$

where $S(z) = z(1 - \tanh^2 z) + \tanh z$.

An approximate solution of the system (1.6) can be obtained for a plain step ($\ell = 0$) if the infinite sums in the representation (1.4), i.e., nonpropagating waves, are disregarded [2]. It is a simple matter to write out the solution of this problem and to determine the coefficients

$$R = \frac{|k_1G^2 - k_2\Lambda_1\Lambda_2|}{k_1G^2 + k_2\Lambda_1\Lambda_2}, \quad T = \frac{2k_1G\Lambda_1 \operatorname{ch} k_2H_2}{k_1G^2 + k_2\Lambda_1\Lambda_2}, \tag{1.8}$$
$$G = k_2 \operatorname{sh} k_2 h / (k_1^2 - k_2^2).$$

In the linear wave approximation ($k_1H_1 \to 0$, $k_2H_2 \to 0$) Eqs. (1.8) give the well-known result $R = (\sqrt{H_2/H_1} - 1)\,(1 + \sqrt{H_2/H_1})$, $T = 2/(1 + \sqrt{H_2/H_1})$. The propagation of waves over an infinite step is investigated in detail in [6].

The interesting characteristic of the wave motion in the case of a step with a water pocket ($\ell \neq 0$) is the kinetic energy of the fluid contained in the pocket. For the rectangular subregion S_3 the kinetic energy, averaged over the wave period and normalized to the length h, is given by the equation

$$E_p = \frac{\rho}{2h} \left\langle \int\limits_{-H_1}^{-H_2} \Phi_3 \frac{\partial\Phi_3}{\partial x}\,dy \right\rangle = \frac{\rho}{8} \sum_{m=1}^{\infty} |C_m|^2 \beta_m \operatorname{ch}\beta_m l \operatorname{sh}\beta_m l$$

(ρ is the density of the fluid, the angle brackets denote time averaging, and the integration is carried out at x = 0). The kinetic energy of the incidence wave, referred to its wavelength $\lambda = 2\pi/k_1$, is $E_w = \rho g a^2/4$. We denote $E = E_p/E_w$.

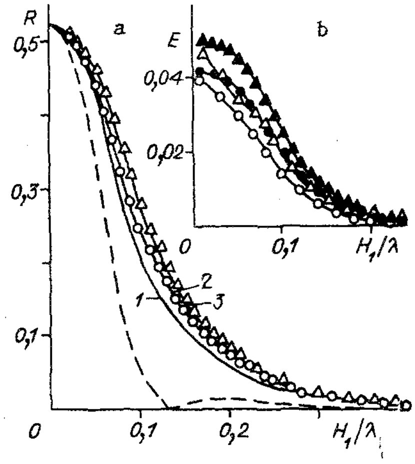

Fig. 2

TABLE 1

N	M	H_1/λ 0,05 R	0,05 $E\cdot10^2$	0,1 R	0,1 $E\cdot10^2$	0,15 R	0,15 $E\cdot10^2$	0,2 R	0,2 $E\cdot10^2$
10	40	0,4601	3,333	0,2851	1,866	0,1519	0,683	0,0797	0,251
15	30	0,4603	3,372	0,2858	1,877	0,1534	0,695	0,0816	0,259
15	40	0,4603	3,387	0,2858	1,884	0,1535	0,699	0,0817	0,261
15	40	0,4595	4,540	0,2826	2,510	0,1501	0,940	0,0793	0,346

The results of numerical calculations of E and the specific kinetic energy E for $H_2/H_1 = 10$ are shown in Table 1 and in Fig. 2. Table 1 illustrates the convergence of the numerical values as a function of the number terms retained in Eqs. (1.4) for $\ell/H_1 = 10$; the top three rows correspond to the case in which the wave is incident on the step from the right, i.e., from the deep-water to the shallow-water part of the fluid (forward step); the last row corresponds to the original statement of the problem (backward step). It has been shown [6] that the reflection coefficients coincide for forward and backward steps when $\ell = 0$. In the given calculations this condition is valid within relative error limits of 2% if both steps have the same value of ℓ. The reflection coefficient is not as sensitive to variations of N and M as the kinetic energy. Figures 2a and 2b show R and E, respectively, for $\ell/H_1 = 0$, 1, 5 (curves 1-3). The light circles and triangles give the values for a forward step, and the dark symbols give the values for a backward step. The calculations are carried out for N = 15 and M = 40. The dashed curve corresponds to the approximation (1.8), which is obviously unacceptable for the given large difference in depths. The reflection coefficient and the kinetic energy for the indicated parameters are almost invariant with a further increase in the dimensions of the water pocket. The presence of this pocket has scarcely any influence on the reflection coefficient for $H_2/H_1 \leq 2$. As H_2 is increased, the maximum specific kinetic energy for fixed values of ℓ and H_1 increases at first to approximately $H_2/H_1 \approx 10$ and then begins to decrease.

2. The flow diagram for wave propagation over a trench is shown in Fig. 1b. The depth of the fluid outside the trench is H_1, the depth in the trench is H_2, the length of its open pore is L, the widths of the left and right water pockets are ℓ_1 and ℓ_2, respectively, and the total width of the trench is $L + \ell_1 + \ell_2$. The vertical axis passes through the left end of the open part of the trench. The incident wave travels from left to right. The flow region S is partitioned into five rectangular subregions: $S_1 = [-\infty < x \leq 0,\ -H_1 \leq y \leq 0]$; $S_2 = [0 \leq x < L,\ -H_2 \leq y \leq 0]$; $S_3 = [L < x < \infty,\ -H_1 \leq y \leq 0]$; $S_4 = [-\ell_1 < x < 0,\ -H_2 \leq y \leq -H_1]$; $S_5 = [L < x < L < \ell_2\ -H_2 \leq y \leq -H_1]$; solutions are sought in each subregion in a form analogous to Eqs. (1.4):

$$\varphi_1 = \varphi_0 + A_0 \exp(-ik_1x) Y_1(y) + \sum_{n=1}^{\infty} A_n \exp(k_{1n}x) Y_{1n}(y),$$

$$\varphi_2 = [D_0 \exp(ik_2x) + F_0 \exp(-ik_2x)] Y_2(y) +$$

TABLE 2

N	H_1/λ							
	0,05		0,1		0,15		0,2	
	T	E	T	E	T	E	T	E
5	0,7728	0,2612	0,9845	0,4125	0,9987	0,2734	0,9993	0,1357
10	0,7728	0,2634	0,9827	0,4148	0,9981	0,2740	0,9995	0,1359
15	0,7726	0,2636	0,9823	0,4148	0,9979	0,2738	0,9995	0,1357
	0,7725	—	0,9802	—	0,9971	—	0,9997	—

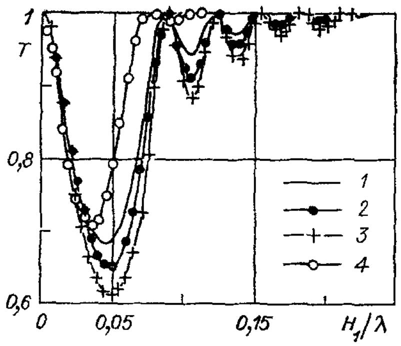

Fig. 3

$$+\sum_{n=1}^{\infty}[D_n\exp(k_{2n}x)+F_n\exp(-k_{2n}x)]\,Y_{2n}(y),$$

$$\varphi_3=B_0\exp(ik_1x)\,Y_1(y)+\sum_{n=1}^{\infty}B_n\exp(-k_{1n}x)\,Y_{1n}(y),$$

$$\varphi_4=C_0+\sum_{m=1}^{\infty}C_m\cos\beta_m(y+H_1)\operatorname{ch}\beta_m(x+l_1),$$

$$\varphi_5=G_0+\sum_{m=1}^{\infty}G_m\cos\beta_m(y+H_1)\operatorname{ch}\beta_m(L+l_2-x). \tag{2.1}$$

The solutions are matched at the vertical segments $x = 0$, $x = L(-H_2 \le y < 0)$. By analogy with Sec. 1, the unknown constants in the representation of the solution for ϕ_4 and ϕ_5 are expressed in terms of the constants of the functions ϕ_1, ϕ_2, and ϕ_3. The original problem is ultimately reduced to the solution of a system of linear algebraic equations of order $4 + 4N$. The convergence of the method for various numbers N is illustrated in Table 1 from [2] in the example of calculations of the reflection and transmission coefficients for a plain trench ($\ell_1 = \ell_2 = 0$) for $H_2/H_1 = 3$ and $L/H_1 = 10$. These results are fully corroborated in the present study.

An alternative method for the analysis of wave diffraction by a trench is given in [7]. A horizontal line segment separates the flow region two subregions: the trench proper and the subregion of constant depth. The solutions are matched at this segment by the collocation method. In the case of a partially capped trench, however, we run into the problem of the stability of the numerical solution for certain parameters of the motion, because the flow has singularities at the corner points (see Sec. 1), which are not essential in integral matching. The error of calculation of the transmission coefficient and energy for several values of N and H_1/λ is shown in Table 2 for $H_2/H_1 = 7.625$, $L/H_1 = 10.59$, and $\ell_1 = \ell_2 = 0$; the last row of the table gives data obtained in [7] for the transmission coefficient when the maximum number of collocation points is 50. We see that the integral method already yields satisfactory results for N = 10.

The kinetic energy of the fluid in the trench, averaged over the wave period and normalized to the length of the "slot" L, is determined by analogy with [8]:

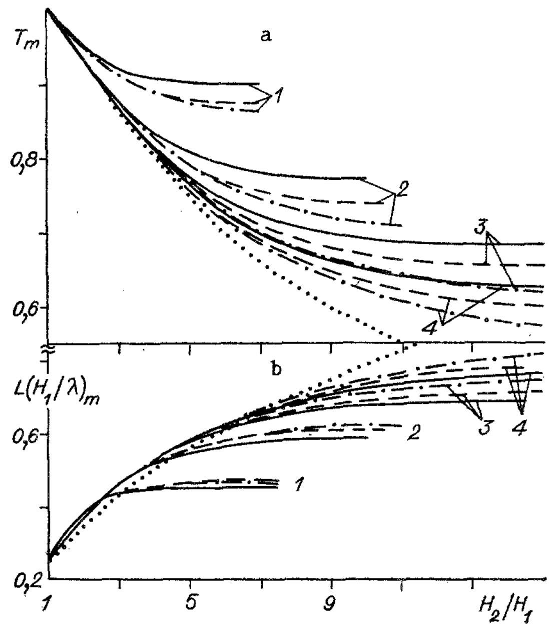

Fig. 4

$$E_p = \frac{\rho}{2L}\left\langle \int_0^L \Phi_2 \frac{\partial \Phi_2}{\partial y}\, dx \right\rangle.$$

The integration is carried out for $y = -H_1$. A detailed investigation of the specific kinetic energy E for a plain trench [8] shows that it depends strongly both on the characteristics of the incident wave and on the geometry of the trench.

Several approximate methods are available for analyzing wave diffraction by a plain trench. The rejection of nonpropagating waves in the expansions (2.1) gives the following expressions for the reflection and transmission coefficients [2]:

$$R^2 = \alpha/(1+\alpha),\ T^2 = 1/(1+\alpha),$$
$$\alpha = [(\gamma^2 - 1)^2/4\gamma^2] \sin^2 k_2 L,\ \gamma = k_1 G^2/k_2 \Lambda_1 \Lambda_2. \qquad (2.2)$$

Letting $k_1H_1 \to 0$ and $k_2H_2 \to 0$, we obtain the long-wavelength approximation [2, 9] from Eqs. (2.2):

$$R = (\sqrt{H_2/H_1} - \sqrt{H_1/H_2}) \sin\theta/d,\ T = 2/d,$$
$$\theta = \sigma L/\sqrt{gH_2},\ d = [4\cos^2\theta + (\sqrt{H_2/H_1} + \sqrt{H_1/H_2})^2 \sin^2\theta]^{1/2}. \qquad (2.3)$$

A more accurate long-wavelength solution is given in [10], where the unknown characteristics are expressed in terms of a single unknown parameter, which is determined numerically. The various approximations have been analyzed and compared with the complete solution in [2], where it is shown, in particular, that the approximation (2.2) gives sufficiently accurate results for relatively small differences in the two depths.

In the small roughness approximation $[(H_2 - H_1)/H_1 \ll 1]$, according to [11],

$$R = \frac{2k_1(H_2 - H_1)|\sin k_1 L|}{2k_1H_1 + \operatorname{sh} 2k_1H_1},$$

$$T = \sqrt{1 + \left[\frac{2(H_2 - H_1)Lk_1^2}{2k_1H_1 + \operatorname{sh} 2k_1H_1}\right]^2}.$$

The energy conservation law (1.7), which has the form $R^2 + T^2 = 1$ for the invstigated flow, is not satisfied here. It has been shown [12] in the example of problems of surface wave generation in a fluid with a rough bottom that the small roughness approximation is applicable only for $H_2/H_1 \leq 1.2$.

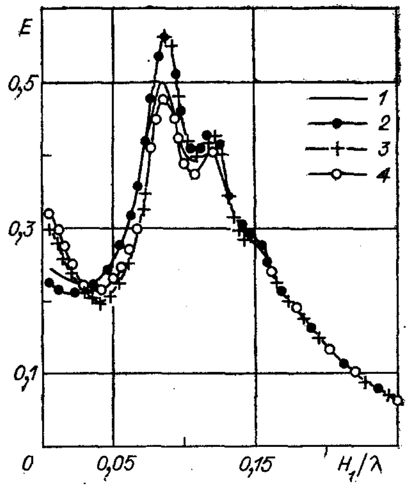

Fig. 5

The dependence of the transmission and reflection coefficients on the wavelength of the incident wave has been investigated in detail for a plain trench [2, 7, 8]. The interesting feature of these dependences is the existence of so-called wave "transparency" (transmission) windows, i.e., discrete values of λ at which the reflection coefficient becomes very small, and the transmission coefficient is close to unity. For the long-wavelength approximation (2.3) this effect occurs at $\lambda = \frac{2L}{n}\sqrt{\frac{H_1}{H_2}}$ $(n = 1, 2, \ldots)$.

The results of numerical calculations of the transmission coefficient for a slotted (partially capped on both sides) trench are given in Fig. 3 for $H_2 = L = 15H_1$, $N = 20$, and $M = 40$; curves 1-3 correspond to the following cases: 1) $\ell_1 = \ell_2 = 0$; 2) $\ell_1 = 0$, $\ell_2 = 10H_1$; 3) $\ell_1 = \ell_2 = 10H_1$. For $\ell_1 = 10H_1$ and $\ell_2 = 0$ the values of T coincide with curve 2. Curve 4 represents the approximate solution (2.2). In the presence of the water sockets S_4 and S_5 the local minima of the reflection coefficient are smaller than in the case a plain trench, and the positions of the extrema of curves 2 and 3 are shifted very slightly toward higher frequencies. This behavior can be explained on the basis of the results of [13], in which it is shown that the natural frequencies of any rectangular region with the same opening L in the upper cap are slightly higher than the natural frequencies of a rectangular region of width L fully open at the top.

Figure 4 shows the variations of the minimum of the transmission coefficient T_m(a) and its position $(H_1/\lambda)_m$ (b) as functions of the depth of the trench H_2 for various values of L, ℓ_1, and ℓ_2. The groups of curves 1-4 correspond to $L/H_1 = 5, 10, 15, 20$. In each group, the solid curve is given for $\ell_1 = \ell_2 = 0$, the dashed curve for $\ell_1 = \ell_2 = H_1$, and the dot-dashed curve for $\ell_1 = \ell_2 = 5H_1$. The dotted curve corresponds to the long-wave approximation (2.3), for which

$$T_m = 2\sqrt{H_1H_2}/(H_1 + H_2),\ (H_1/\lambda)_m = \sqrt{H_1H_2}/4L. \tag{2.4}$$

We see that one of the governing parameters for wave propagation over a trench is the length of its open part and that the greater this length, the greater is the range of depths H_2 for which Eqs. (2.4) are valid. Beginning with a certain depth H_2 (which increases with L), a further increase in the depth of the trench has scarcely any effect on the characteristics of the wave motion. The influence of the water pockets is very weak for relatively small lengths L ($L/H_1 \leq 5$) and increases slightly with L. The maximum decrease of T_m is not very appreciable in this case and is already attained at ℓ_1, $\ell_2 \approx 5H_1$. A further increase in ℓ_1 or ℓ_2 has little influence on the wave motion. The transmission coefficient becomes equal to zero in the limit L, $H_2 \to \infty$, which corresponds to an infinite step [6].

The variation of the specific kinetic energy trapped in the trench is shown in Fig. 5 for the same values of the parameters as in Fig. 3. Curves 1-3 are analogous to those in Fig. 3, and curve 4 corresponds to $\ell_1 = 10H_1$ and $\ell_2 = 0$. We note that the distribution of E depends very slightly on the parameters ℓ_1 and ℓ_2. As remarked previously [8], the function E has local maxima near the transparency windows. The occurrence of these maxima indicates the resonance response of the trench to the incidence of waves having a certain wavelength.

The author thanks S. V. Sukhinin for discussing the results of this work.

LITERATURE CITED

1. V. S. Ermakov, I. S. Nudner, and L. S. Nudner, "Influence of waves on a rectangular obstacle submerged in a fluid," Vod. Resursy, No. 4 (1978).
2. J. T. Kirby and R. A. Dalrymple, "Propagation of obliquely incident water waves over a trench," J. Fluid Mech., 133 (1983).
3. F. C. K. Ting and F. Raichlen, "Wave interaction with rectangular trench in density-stratified fluid," J. Waterway Port Coastal Ocean Eng., 114, No. 5 (1988).
4. G. V. Simakov, I. S. Nudner, and V. V. Belov, "Investigations of wave propagation over underwater obstacles," in: Hydraulic Engineering Installations [in Russian] (inter-university collection), DVPI, Vladivostok (1985).
5. J. V. Wehausen and E. V. Laitone, "Surface waves," in: Handbuch der Physik, Vol. 9: Strömungsmechanik III, Berlin (1960).
6. J. N. Newman, "Propagation of water waves over an infinite step," J. Fluid Mech., 23, Part 2 (1965).
7. J.-J. Lee and R. M. Ayer, "Wave propagation over a rectangular trench," J. Fluid Mech., 110 (1981).
8. F. C. K. Ting and F. Raichlen, "Wave interaction with a rectangular trench," J. Waterway Port Coastal Ocean Eng., 112, No. 3 (1986).
9. M. V. Babii and L. V. Cherkesov, "Influence of an underwater obstacle on the deformation of long waves," in: Ocean Hydrophysical Research [in Russian], No. 2, Mor. Gidrofiz. Inst. Akad. Nauk UkrSSR (1973).
10. J. W. Miles, "Surface-wave diffraction by a trench," J. Fluid Mech., 115 (1982).
11. C. C. Mei, "Weak reflection of water waves by bottom obstacles," Proc. ASCE J. Eng. Mech. Div., 95, No. 1 (1969).
12. B. E. Protopopov and I. V. Sturova, "Generation of plane surface waves in the presence of small bottom roughness," Zh. Prikl. Mekh. Tekh. Fiz., No. 1 (1989).
13. D. W. Fox and J. R. Kuttler, "Sloshing frequencies," Z. Angew. Math. Phys., 34, No. 5 (1983).